

The Influence of Microstructure on the Mechanical Behaviour of Dual Phase Steels

R. Amaral, A.D. Santos, J.A. Sousa and A.B. Lopes

1 Introduction

Transportation industry and particularly the automotive industry is facing in the coming future a number of challenges, including more stringent legislation on efficiency, fuel consumption, emissions and safety. These requests include the need to reduce the weight of automobiles and improvement of aspects related to safety and security. These issues are related and involve the selection and use of appropriate materials with higher strength properties, so that thinner components will have similar or better characteristics to previous thicker parts with additional weight. Other important material properties include high energy absorption and good formability behaviour, in order to obtain the component with the required geometry.

Among high-strength materials, dual phase (DP) steels are very important engineering materials due to their exceptional combination of high strength and

R. Amaral (✉) · A.D. Santos
INEGI, Institute of Science and Innovation in Mechanical
and Industrial Engineering, R. Dr. Roberto Frias, 400, 4200-465 Porto, Portugal
e-mail: ramaral@inegi.up.pt

A.D. Santos
e-mail: abel@fe.up.pt

A.D. Santos
FEUP, Faculty of Engineering, University of Porto, R. Dr. Roberto Frias,
4200-465 Porto, Portugal

J.A. Sousa · A.B. Lopes
CICECO Aveiro Institute of Materials, Department of Material
and Ceramic Engineering, University of Aveiro,
Campus Universitário de Santiago, 3810-193 Aveiro, Portugal
e-mail: joseandrealvessousa@gmail.com

A.B. Lopes
e-mail: augusto@ua.pt

good formability thus allowing the production of both thin and strong components for many applications. The microstructure of these advanced high strength steels (AHSS), which are currently used in automotive industry, is predominantly composed by a soft ferritic matrix, that ensures the good formability, combined with hard martensite particles acting as a strengthening phase [1, 2].

On the other hand, the use of numerical methods is today a basic requirement when analyzing manufacturing processes, such as sheet metal forming. The corresponding advantages include the possibilities to improve processing and the quality of final product, as well as permitting an evident increase in efficiency both for time and cost reductions. However, the accuracy of numerical analysis of the plastic forming operations depends on a correct characterization of material properties.

During metal forming operations the material is usually loaded under different strain paths, which may change along the process and most probably will affect its formability limits by promoting damage or necking and thus leading to rejection of the product.

Mechanical behaviour of material is defined in each instant by the evolution of dislocation structures and crystallographic textures, which in turn will depend on different parameters like crystal structure, presence of solutes or second phases, loading path, pre-strain values, amplitude of the strain path change, etc. [3, 4].

Although its extensive use, the behaviour of dual phase steels has still many questions to be solved, particularly the effect of martensitic hard particles on the evolution of dislocation structures and crystallographic textures.

This chapter presents a study on the mechanical and microstructural behaviour of dual phase steels sheets with different amounts of martensite. The mechanical behaviour was characterized by tensile tests along different orientations in respect to rolling direction of the sheets.

Also, the mechanical behaviour exhibited by material during these tests was analyzed in terms of dislocation microstructure and crystallographic texture evolutions using scanning electron microscopy (SEM), electron backscattered diffraction (EBSD), nanoindentation tests and calculations with viscoplastic self-consistent (VPSC) model proposed by Lebensohn and Tome [5].

2 Microstructural Characterization

The materials used in this work were three DP steels sheets with 0.8 mm thickness and different amounts of martensite, namely DP500, DP600 and DP780.

The SEM observations performed on the initial materials (Fig. 1) showed that the microstructure is defined by the presence of hard martensite particles (white areas) dispersed in the soft ferritic matrix.

The average size of ferritic grains and volume percentage of martensite for each dual phase steel, obtained from microstructural observations are presented in Table 1.

Nanoindentation tests performed in different points (Fig. 2) showed that materials present very different hardness values along the analyzed areas, corresponding

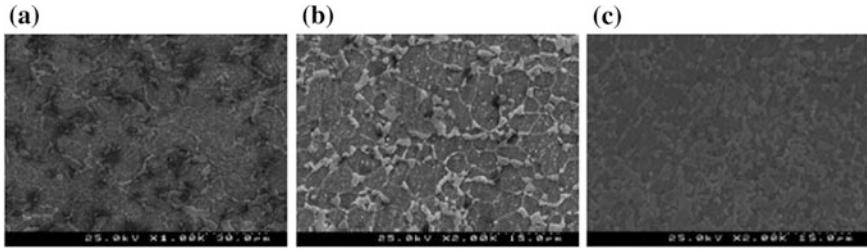


Fig. 1 SEM images of initial materials **a** DP500, **b** DP600 e **c** DP780

Table 1 Average size of ferritic grains (D) and volume percentage of martensite (V_M) for the initial materials

Material	D (μm)	V_M (%)
DP500	22	13
DP600	10	18
DP780	6	25

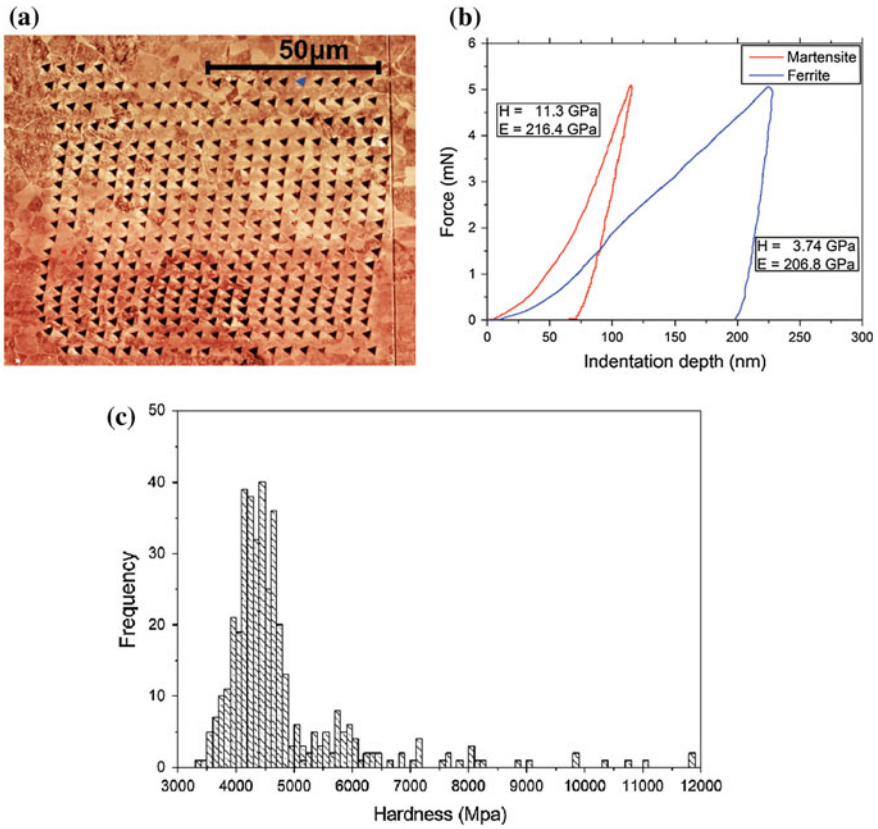


Fig. 2 Results of nanoindentation tests in different points of the sample (DP500); **a** image obtained by atomic-force microscopy (AFM) for the area under analysis; **b** curves force-penetration for the higher and lower hardness points; **c** frequency histogram for hardness values

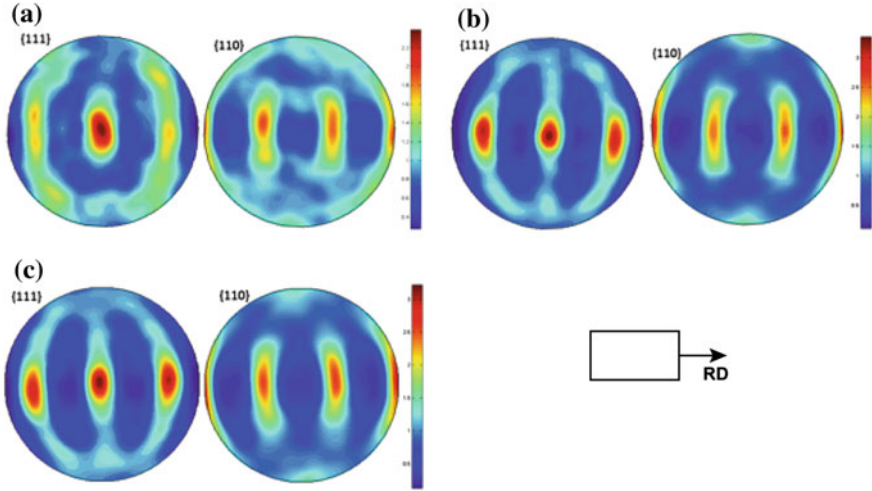


Fig. 3 Experimental pole figures $\{111\}$ and $\{110\}$ from initial materials. **a** DP500; **b** DP600; **c** DP780. RD—rolling direction of the sheet

to different phases: martensite having a high hardness and ferrite with a much lower hardness value.

Pole figures from ferritic grains obtained by EBSD (Fig. 3) show the existence of a γ fiber ($\{111\} \langle uvw \rangle$) type crystallographic texture with a reinforcement of the $\{111\} \langle 110 \rangle$ component, which is typical of rolled steel sheets [6].

3 Mechanical Characterization

3.1 Uniaxial Tensile Test

Uniaxial tensile tests were performed at room temperature using a machine crosshead speed of 5 mm/s, which corresponds to an initial strain rate of 0.0016 s^{-1} . Specimens were machined according to ASTM E 8M-04 standard and the tests were performed for three different directions relative to the rolling direction (0° , 45° and 90°). Results were averaged from three experiments for each direction and material, in order to test and ensure repeatability. Figure 4 shows the corresponding stress-strain hardening curves for each DP steel and direction.

The obtained mechanical parameters extracted from curves along the rolling direction of the sheets are presented in Table 2, namely yield stress ($R_{p0.2}$), ultimate tensile strength (R_m), elongation at yield point (e_0), uniform elongation (e_u) and total elongation (e_t).

The anisotropy coefficient (r) for different angles to the rolling direction has been measured (Fig. 5). It is noticed the two different evolution behaviours presented by

Fig. 4 Results from tensile test for true stress-strain curves of dual phase steels along three different directions 0°, 45° and 90° to rolling direction

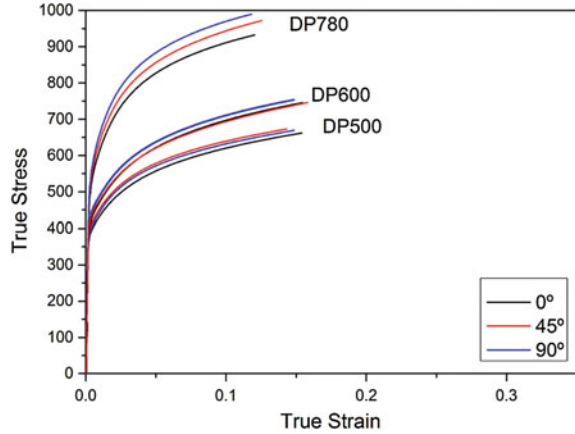


Table 2 Mechanical properties for dual phase steels under current study, along rolling direction

Material	$R_{p0.2}$ (MPa)	R_m (MPa)	e_0 (%)	e_u (%)	e_t (%)
DP500	356.53	544.84	0.34	18.18	29.52
DP600	416.05	630.85	0.37	16.40	27.14
DP780	526.18	843.10	0.47	12.53	17.96

the three materials. The DP500 has the lowest r-value at 45° to the rolling direction, while the pair DP600/DP780 show the highest value for such direction. All of them have higher r-values for transverse direction (90°) when compared to rolling direction (0°).

By using the experimental crystallographic texture of initial materials as input of VPSC model [5] it was possible to predict the evolution of anisotropy coefficient (Fig. 6) for different angles to rolling direction. The obtained results showed that

Fig. 5 Evolution of anisotropy coefficients along different angles to rolling direction

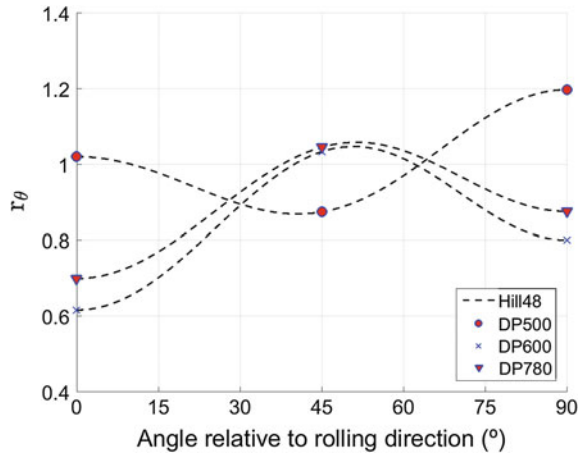
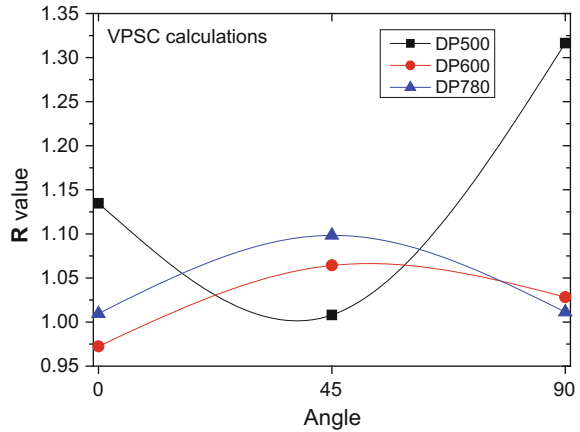


Fig. 6 Predicted anisotropy coefficients by VPSC model along different angles to rolling direction



both the simulated and experimental values present a similar evolution, thus giving evidence on the relation between initial crystallographic texture and initial anisotropy exhibited by materials.

3.2 Hydraulic Bulge Test

A biaxial hydraulic bulge test has been used with a tactile mechanical system (Fig. 7) to obtain biaxial stress-strain curve. The experimental system is composed by a set of tools, a hydraulic pump and a tactile mechanical device, which is in contact with sheet blank and permits to obtain data acquisition about specimen curvature and elongation at the pole, thus getting the relevant information for material characterization by coupling it with membrane theory.



Fig. 7 Experimental system used for biaxial hydraulic bulge test

Table 3 Mechanical properties for dual phase steels obtained from biaxial hydraulic bulge test

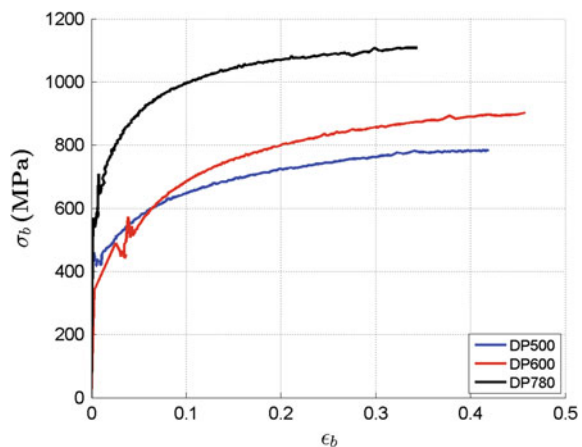
Material	Burst pressure (bar)	Total height at pole w/fracture (mm)
DP500	87.21	49.52
DP600	97.62	50.05
DP780	119.61	42.04

The set of tools contains a circular die, with a nominal diameter of 150 mm and die radius of 13 mm, as well as a blank holder with a drawbead, which restrains the sample and avoids any oil leakage during the test. The measuring system is calibrated before each test in order to ensure accuracy and reproducibility of data acquisition. The bulge test is performed with a pressure increment of 1 bar/s and the diameter of circular samples is 250 mm. The experimental system [7] allows the continuous acquisition of hydraulic pressure (p), as well as the variables provided by the measuring system: radius of curvature (ρ) and biaxial strain (ϵ). The ratio blank diameter/thickness permits the application of the membrane theory, which gives the evolution of material hardness behaviour for biaxial stress versus strain.

Table 3 presents the results obtained for maximum pressure (burst) obtained in biaxial hydraulic bulge test for each material, as well as the corresponding total height at the pole.

Results obtained for hardening biaxial stress-strain curves for each of DP steels from bulge test are shown in Fig. 8. Some oscillations (irregular behaviour) are observed for very low values of strain, which is due to variations for high levels of blank curvature (almost flat blank corresponds to an almost infinite radius of curvature) and low values of hydraulic pressure. Also, Fig. 8 shows that a similar initial yield stress for DP500 and DP600 exists, although DP600 has a higher strength evolution with continuing deformation, as expected.

Fig. 8 Biaxial stress-strain curves for dual phase steels, obtained by hydraulic bulge test



3.2.1 Biaxial Stress-Strain Curve Conversion to Equivalent Stress-Strain Curve

By performing tensile and hydraulic bulge mechanical tests, one obtains two hardening curves for the same material, from each test. Defining that curve $\sigma = f(\varepsilon)$ corresponds to the uniaxial tensile test (along rolling direction) and curve $\sigma_b = f(\varepsilon_b)$ corresponds to hydraulic bulge test, one should have the same work performed to deform material, since the material is the same, therefore one should have a common hardening curve. However, the two hardening curves may not be coincident, since they don't belong to the same space of deformation and therefore the biaxial curve must be converted to the equivalent stress-strain curve.

The conversion of the biaxial stress-strain curve into the equivalent stress-strain curve, will be based on the principle of equivalent plastic work. In this way, assuming the incompressibility of the material and considering the state of stress at the pole as $\sigma_1 = \sigma_2 = \sigma_b$, one can reshape the relationship of equivalent plastic work ($\sigma \cdot \varepsilon = \sigma_1 \cdot \varepsilon_1 + \sigma_2 \cdot \varepsilon_2$) by using Levy-von Mises and therefore Eq. 1 is obtained:

$$\frac{\sigma}{\sigma_b} + \frac{\varepsilon_b}{\varepsilon} = k \quad (1)$$

where k is a constant.

The equivalent plastic work is the link between the two curves, being W_u the plastic work per unit volume for the tensile test and W_b for the hydraulic bulge test. This methodology has been also used by other authors with corresponding satisfactory results [8–10].

Integrating $\sigma = f(\varepsilon)$ for the overall plastic domain one obtains the corresponding plastic work per volume unit for both tests, Eq. 2:

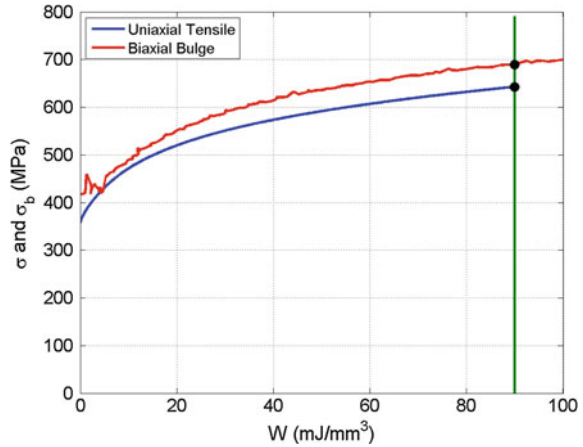
$$W(\varepsilon) = \int_{i=i(\varepsilon_i)}^{i=i(\varepsilon_f)-1} (\varepsilon_{i+1} - \varepsilon_i) \cdot \frac{\sigma_{i+1} + \sigma_i}{2} \quad (2)$$

When $W_u = W_b$ it is possible to establish a relationship between the stresses or strains for both tests, i.e.:

$$\begin{cases} \sigma \rightarrow W_u = W_b = \sigma_b \\ \varepsilon \rightarrow W_u = W_b = \varepsilon_b \end{cases} \quad (2)$$

To obtain k parameter, several methods can be considered [8, 9, 11]. In this chapter, it will be used a method based on the equivalent plastic work, by corresponding to the maximum values of stress and strain for the uniaxial tensile test ($\sigma_{max} \rightarrow W_u = W_b \rightarrow \sigma_b \Rightarrow k_l = \sigma_{max}/\sigma_b$), as shown in Fig. 9 [9].

Fig. 9 Relation between plastic work and stress obtained from each test (tensile, bulge) by using the maximum stress from tensile test



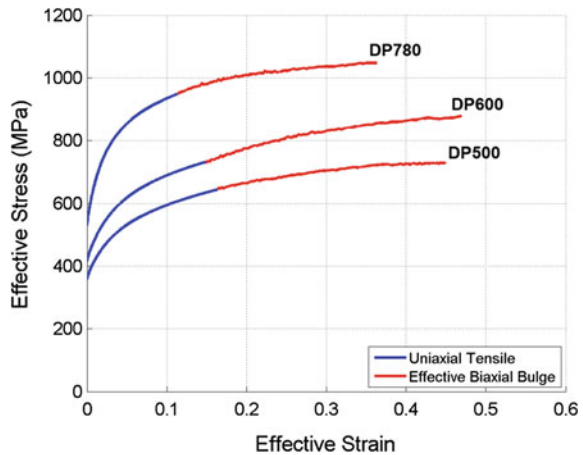
In Table 4 it is shown the corresponding values for k parameter used to convert biaxial stress-strain curve into equivalent stress-strain curve, by using the defined method of maximum values of stress and strain from uniaxial tensile test.

The final result of converting biaxial data and including it in the equivalent hardening curve is presented in Fig. 10, for every dual phase steel. It is observed

Table 4 k parameter used to convert biaxial stress-strain curve into equivalent stress-strain curve, for each dual phase steel

Parameter	Material		
	DP500	DP600	DP780
k	0.9318	0.9645	0.9423

Fig. 10 Combination of stress-strain curve from tensile test with biaxial stress-strain curve, based on the principle of equivalent work and method of maximum values of stress and strain from uniaxial tensile test



that using the selected method there is a good first derivative continuity for the extension of hardening curve based on bulge test, both for DP500 and DP780. As for DP600 there is a less perfect continuity in the transition between tensile data and bulge data, although being still very smooth and having a good overall behaviour.

4 Conclusions

Three dual-phase steels with different amounts of martensite (DP500, DP600 and DP780) were selected and investigated for characterization and analysis of mechanical and microstructural analysis.

The incompatibilities of deformation between soft ferritic matrix and the hard martensite particles promotes a very inhomogeneous plastic deformation of the ferrite grains and the selected dual-phase steels sheets show an anisotropic behaviour for monotonic tensile tests, which is due and related to their initial crystallographic texture. The corresponding relation and prediction has been performed by a VPSC (viscoplastic self-consistent) model and its results show a good agreement with the experiments.

The conversion of bulge data to the equivalent stress-strain hardening curve by using the method of maximum values of stress and strain from uniaxial tensile test has shown to provide a good correlation, in order to obtain the extension of hardening information for selected dual phase steels, thus giving possibility of material characterization for higher strain values based on experimental data.

Acknowledgements The authors would like to acknowledge the support of this work by FEDER funds through the Operational Program for Competitiveness Factors (COMPETE) and by national funds through the FCT (Foundation for Science and Technology) through the projects PTDC/EMS-TEC/2404/2012, POCI-01-0145-FEDER-016876 and PTDC/EMS-TEC/6400/2014.

References

1. Kim, S.B., Huh, H., Bok, H.H., Moon, M.B.: Forming limit diagram of auto-body steel sheets for high-speed sheet metal forming. *J. Mater. Proc. Technol.* **211**, 851 (2011)
2. Cao, Y., Karlsson, B., Ahlström, J.: Temperature and strain rate effects on the mechanical behavior of dual phase steel. *Mater. Sci. Eng. A* **636**, 124–132 (2015)
3. Lopes, A.B., Barlat, F., Gracio, J.J., Duarte, J.F.F., Rauch, E.F.: Effect of texture and microstructure on strain hardening anisotropy for aluminum deformed in uniaxial tension and simple shear. *Int. J. Plast.* **19**, 1 (2003)
4. Vincze, G., Rauch, E.F., Gracio, J.J., Barlat, F., Lopes, A.B.: A comparison of the mechanical behaviour of an AA1050 and a low carbon steel deformed upon strain reversal. *Acta Mater.* **53**, 1005 (2005)
5. Lebensohn, R.A., Tome, C.N.: *Acta Metall. Mater.* **9**, 2611 (1993)
6. Rollett, A.D., Wright, S.I.: In: Kocks, U.F., Tome, C.N., Wenk, H.R. (eds.), *Texture and Anisotropy: Preferred Orientations in Polycrystals and Their Effect on Materials Properties*, p. 178. Cambridge University Press (1998)

7. Campos, H., Santos, A.D., Martins, B., Ito, K., Mori, N., Barlat, F.: Hydraulic bulge test for stress-strain curve determination and damage calibration for Ito-Goya model. In: 11th World Congress on Computational Mechanics, 5th European Conference on Computational Mechanics and 6th European Conference on Computational Fluid Dynamics, pp. 4223–4238 (2014)
8. Mutrux, A., Hochholdinger, B., Hora, P.: Procedure for evaluation and validation of hydraulic biaxial experiment. In: Numisheet 2008, Switzerland, pp. 67–71 (2008)
9. Sigvant, M., Mattiasson, K., Vegter, H., Thilderkvist, P.: A viscous pressure bulge test for determination of a plastic hardening curve and equibiaxial material data. *Int. J. Mater. Form.* **2**, 235–242 (2009)
10. Lazarescu, L., Nicodim, I., Ciobanu, I., Comsa, D.S., Banabic, D.: Determination of material parameters of sheet metals using the hydraulic bulge test. *Acta Metall. Slovaca* **19**(1), 4–12 (2013)
11. Lee, M.-G., Kim, D., Kim, C., Wenner, M.L., Wagoner, R.H., Chung, K.: Springback evaluation of automotive sheets based on isotropic-kinematic hardening laws and non-quadratic anisotropic yield functions—Part II: characterization of material properties. *Int. J. Plast.* **21**, 883–914 (2005)